JAIST Repository
https://dspace.jaist.ac.jp/

Title	A low-temperature crystallization path for device-quality ferroelectric film
Author(s)	Li, Jinwang; Kameda, Hiroyuki; Trinh, Bui Nguyen Quoc; Miyasako, Takaaki; Tue, Phan Trong; Tokumitsu, Eisuke; Mitani, Tadaoki; Shimoda, Tatsuya
Citation	Applied Physics Letters, 97(10): 102905-1-102905-3
Issue Date	2010-09-10
Type	Journal Article
Text version	publisher
URL	http://hdl.handle.net/10119/9897
Rights	Copyright 2010 American Institute of Physics. This article may be downloaded for personal use only. Any other use requires prior permission of the author and the American Institute of Physics. The following article appeared in Jinwang Li, Hiroyuki Kameda, Bui Nguyen Quoc Trinh, Takaaki Miyasako, Phan Trong Tue, Eisuke Tokumitsu, Tadaoki Mitani, and Tatsuya Shimoda, Applied Physics Letters, 97(10), 102905 (2010) and may be found at http://link.aip.org/link/doi/10.1063/1.3486462
Description	

JAPAN
ADVANCED INSTITUTE OF
SCIENCE AND TECHNOLOGY

Japan Advanced Institute of Science and Technology

APPLIED PHYSICS LETTERS **97**, 102905 (2010)

A low-temperature crystallization path for device-quality ferroelectric films

Jinwang Li (李金望),[1,a)] Hiroyuki Kameda (亀田博之),[1,2] Bui Nguyen Quoc Trinh,[1]
Takaaki Miyasako (宮迫毅明),[1] Phan Trong Tue,[3] Eisuke Tokumitsu (徳光永輔),[1,4]
Tadaoki Mitani (三谷忠興),[1] and Tatsuya Shimoda (下田達也)[1,3]
[1]*Japan Science and Technology Agency (JST), ERATO, Shimoda Nano-Liquid Process Project, 2-5-3 Asahidai, Nomi, Ishikawa 923-1211, Japan*
[2]*Electronic Materials Development Laboratory, ADEKA Corporation, 7-2-34 Higashi-ogu, Arakawa-ku, Tokyo 116-8554, Japan*
[3]*School of Materials Science, Japan Advanced Institute of Science and Technology, 1-1 Asahidai, Nomi, Ishikawa 923-1292, Japan*
[4]*Precision and Intelligence Laboratory, Tokyo Institute of Technology, 4259-R2-19 Nagatsuta, Midori-ku, Yokohama 226-8503, Japan*

(Received 15 July 2010; accepted 13 August 2010; published online 10 September 2010)

We show a path for low-temperature crystallization of device-quality solution-processed lead zirconate titanate films. The essential aspect of the path is to circumvent pyrochlore formation at around 300 °C during temperature increase up to 400 °C. By maintaining enough carbon via pyrolysis at 210 °C, well below the temperature for pyrochlore formation, Pb^{2+} can be reduced to Pb^0. This leads to the lack of Pb^{2+} in the film to suppress the development of pyrochlore, which accounts for the usual high-temperature conversion to perovskite. Films on metal, metal/oxide hybrid, and oxide bottom electrodes were successfully crystallized at 400–450 °C. © *2010 American Institute of Physics*. [doi:10.1063/1.3486462]

For the fabrication of high-density ferroelectric nanodevices and their integration with silicon-based CMOS circuits, low-temperature (≤ 450 °C) processing of ferroelectric films is required.[1] Lead zirconate titanate (PZT) is the first choice of ferroelectric materials[2] because of its excellent properties and relatively low processing temperatures (usually 600–700 °C) compared to the other two major options, strontium bismuth tantalate (≥ 700 °C) (Ref. 3) and bismuth lanthanum titanate (≥ 650 °C).[4]

A process appropriate for industrial production of high-quality PZT films at ≤ 450 °C has been sought after for long but without success. Although the chemical vapor deposition technique has been able to grow high-quality PZT films below 500 °C,[5] costs of the complicated facilities and processing are prohibitively high for industrial applications. The chemical solution deposition (CSD) technique is industrially favorable. Many low-temperature CSD methods, including tailoring precursor solution,[6–9] seeding the film,[10,11] hydrothermal annealing,[12,13] and better lattice matching,[14] have been investigated, but all provide insufficient film quality and compromised properties. Hitherto, the relatively successful approaches have been microwave heating (450 °C) (Refs. 15 and 16) and localized heating by pulsed laser at low substrate temperatures (250–400 °C).[1] Nevertheless, microwave heating results in damage of CMOS circuits, while the costly pulsed laser processing is unfavorable for industrial application. In addition, both processes produced films of random orientation instead of the optimal (111) orientation. It should be noted that high oxygen-pressure processing (2–8 MPa, 400 °C)[17,18] succeeded in crystallizing sputtered PZT, whereas it failed for CSD PZT. Further, the use of high pressure is commercially unfavorable. Ultraviolet (UV) excimer light-assisted annealing (450 °C) (Ref. 19) produced randomly oriented $Pb_{1-x}Ca_xTiO_3$ films from precursors containing UV light-absorbing ligands but was not used for PZT. One may expect a higher crystallization temperature after the involvement of zirconium, as often observed.[20] It is also worth pointing out that, regarding the hydrothermal deposition technique, though capable of growing epitaxial lead titanate on oxide substrates,[21] its harsh chemical conditions would erode silicon substrates.

Here we report a simple method for the crystallization of solution-processed PZT films at 400–450 °C on metal, metal/oxide hybrid, and oxide bottom electrodes. Our approach, extended from our study of PZT powders (to be published elsewhere), does not need any modification of the precursors nor special facilities. (See Ref. 22 for the details of experimental methods.) The success lies in the intrinsic change in the crystallization path through circumventing the formation of pyrochlore structure. In conventional CSD studies, in order to completely remove organic components, the spin-coated films are pyrolyzed at over 300 °C, at which temperatures, however, the pyrochlore structure is also developed. In contrast, we intentionally retained an appropriate amount of carbon in the film by partially pyrolyzing at a low temperature of 210 °C, well below the temperature for the development of the pyrochlore structure. The effect of pyrolysis temperature on carbon content was confirmed by second ion mass spectroscopic (SIMS) analysis for a PZT film (90 nm thick) of Pb/Zr/Ti=115/37/63 on (111) Pt [Fig. 1(a)]. The remaining carbon resulted in the reduction of Pb^{2+} to Pb^0 when heated up in subsequent annealing [Figs. 1(b) and 1(c)]. The 210 °C-pyrolyzed sample, after being heated (10 K/min in N_2) to 400 °C, showed a significantly higher amount of reduced Pb than other films pyrolyzed at 280 and 320 °C, as indicated by the peak intensities of $PbPt_x$ (formed at PZT/Pt interface) in the x-ray diffraction (XRD) patterns [Fig. 1(b)] and calculated from x-ray photoelectron spectroscopy (XPS) spectra [Fig. 1(c)]. Note that increasing

---

[a)] Author to whom correspondence should be addressed. Electronic mail: lijw@jaist.ac.jp.

© 2010 American Institute of Physics

Downloaded 12 Sep 2010 to 150.65.164.25. Redistribution subject to AIP license or copyright; see http://apl.aip.org/about/rights_and_permissions

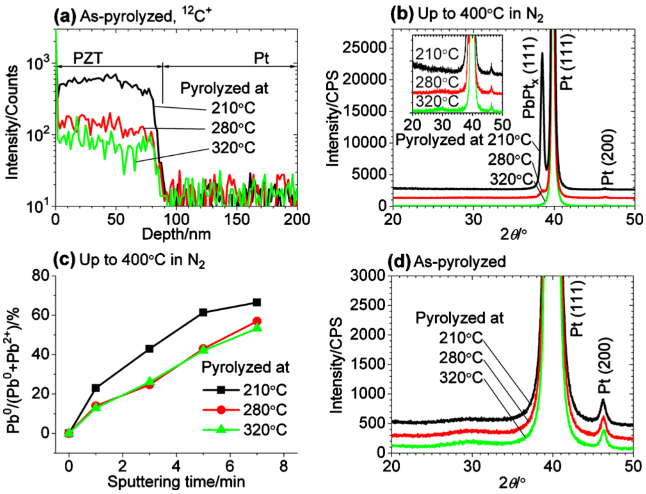

FIG. 1. (Color online) Effects of pyrolysis temperature on carbon content, valence state of Pb, and phase composition before perovskite crystallization. (a) SIMS analysis for carbon of the as-pyrolyzed samples. (b) XRD patterns for samples further heated (10 K/min in N$_2$) to 400 °C and held 1 min. The inset shows the difference of pyrochlore lines ($2\theta=25^\circ-35^\circ$) at expanded intensities. (c) Percentages of reduced Pb, calculated from XPS spectra, as a function of Ar ion sputtering time, for the samples shown in panel (b). (d) XRD patterns for the as-pyrolyzed samples, showing increasing pyrochlore lines ($2\theta=25^\circ-35^\circ$) with increasing pyrolysis temperature. The films were spin-coated three times (90 nm thick after complete removal of organics) on (111) Pt.

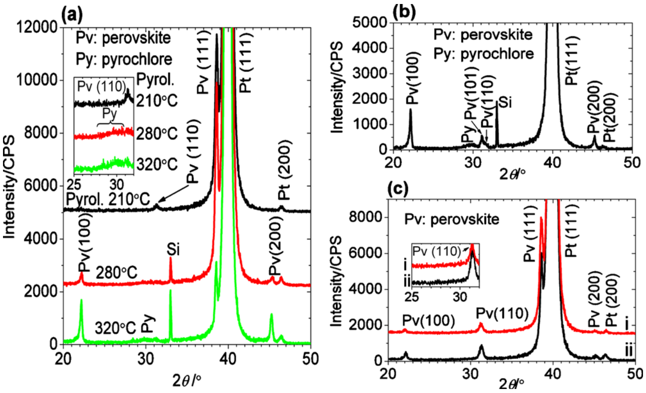

FIG. 2. (Color online) XRD patterns for samples crystallized at 400–450 °C. (a) Three samples pyrolyzed at different temperatures (210 °C, 280 °C, and 320 °C, respectively) but annealed under the same conditions (first in N$_2$, heated at 10 K/min to 400 °C, held 1 min, followed by fast heating at 20 K/s to 450 °C; and then in air, held for 10 h). (b) A 210 °C-pyrolyzed sample heated (10 K/min) in O$_2$, instead of N$_2$, up to 500 °C and held, indicating the failure to keep the Pb^0 state led to poor crystallization of perovskite and a significant presence of pyrochlore. (c) Two 210 °C-pyrolyzed samples (last spin-coated layer only dried at 100 °C) heated up at 20 K/s in N$_2$, and then held in air at (i) 450 °C for 1 h or (ii) 400 °C for 10 h. The insets in panels (a) and (c) show expanded intensities in the range of $2\theta=25^\circ-32^\circ$, where the pyrochlore line appears. All the films were 90 nm thick.

Pb^0 at greater depth [longer argon ion sputtering time, Fig. 1(c)] suggests reasonable faster escape of organic components from the surface during heating. In the presence of sufficient organic carbon, Pb^{2+} is reduced to Pb^0 at temperatures as low as 200 °C. As a result, upon heating up in N$_2$ to the temperature where pyrochlore structure forms (~300 °C), the lack of Pb^{2+}, as in the 210 °C-pyrolyzed sample, prevented the development of this intermediate structure [see the XRD patterns in Fig. 1(b) inset and Fig. 1(d)] that accounts for the high-temperature crystallization of the ferroelectric perovskite phase in the conventional processes. Increasing the pyrolysis temperature to 280 and 320 °C led to insufficient remaining carbon, and the formation of a rather stable pyrochlore structure [as indicated by the more defined lines at $2\theta=25^\circ-35^\circ$ in Fig. 1(d)] that remained during subsequent heating in N$_2$ [Fig. 1(b) inset] and after the final heating in air for perovskite crystallization [Fig. 2(a) inset shown below].

The samples heated (10 K/min in N$_2$) to 400 °C were further heated (20 K/s in N$_2$) to 450 °C and held 10 h in air for reoxidation of the reduced Pb and crystallization of perovskite. The 210 °C-pyrolyzed film developed into well-crystallized (111)-oriented perovskite [Fig. 2(a)]. Increasing the pyrolysis temperature led to increased pyrochlore amount, decreased (111) orientation, and a reduced amount of perovskite phase. The protection with N$_2$ against oxidation is essential for such thin (90 nm) films heated at a slow rate (10 K/min). When the N$_2$ atmosphere was changed to O$_2$, even annealed at 500 °C, the sample was poorly crystallized with a significant amount of pyrochlore [Fig. 2(b)].

Further process optimization indicated that rapid heating (20 K/s in N$_2$) before annealing (450 °C in air) was better. For 90 nm thick samples, the annealing period was reduced to 1 h. It is likely that slow heating led to the excessive reduction of lead, and to damage of the bottom Pt electrode because of excessive reaction with the reduced Pb. In addition, crystallization was improved when the last spin-coated layer (30 nm thick) was not heated to 210 °C, but only to 100–150 °C to maintained more carbon, in order to compensate for faster escape of carbon near the surface. The optimization led not only to well-crystallized films at 450 °C for 1 h [Fig. 2(c), (i)] but also further decreased the crystallization temperature down to 400 °C [Fig. 2(c), (ii)]. Furthermore, for films as thick as 210 nm, the use of N$_2$ in fast heating (20 K/s) was no longer essential. Instead, heating only in air was sufficient because the thicker films protected the inner layer well for a short time against oxidation.

Our process was demonstrated on several representative low-temperature electrode materials (Au, hybrid Pt/RuO$_2$, and RuO$_2$) in addition to Pt, all prepared below 150 °C by sputtering. The film properties (Fig. 3) are similar to or exceed those of high-temperature PZT. The 210 nm thick film (sample 3) on Pt had excellent polarization and leakage properties but the 90 nm thick films (samples 1 and 2) possessed inadequate properties because of film instability at less than 100 nm thick.[23] The film on Au (sample 4) also showed good properties. Au has electrical resistivity (22 nΩ m) five times lower than Pt (105 nΩ m), and is easier to etch for patterning, but previously was not used for thin (~200 nm) PZT films, probably because of interdiffusion in a high-temperature process. Even though thick (>1 μm) PZT films on gold would suffer fewer effects of interdiffusion, the use has been rare.[24] Similar to high-temperature films on Pt,[25] our films on both Pt and Au showed poor fatigue resistance (~10^6 cycles). To improve the fatigue resistance, RuO$_2$ electrodes were used, and the film was well crystallized when the Zr/Ti ratio was decreased to 30/70, and the film was buffered with a 30 nm thick layer of Zr/Ti=20/80 to facilitate nucleation, though with lower (111) orientation than on Pt. The 210 nm thick film (sample 5) showed excellent polarization and fatigue-free properties, but had a high leakage current that was probably due to nonuniform nucleation in crystalli-

Downloaded 12 Sep 2010 to 150.65.164.25. Redistribution subject to AIP license or copyright; see http://apl.aip.org/about/rights_and_permissions

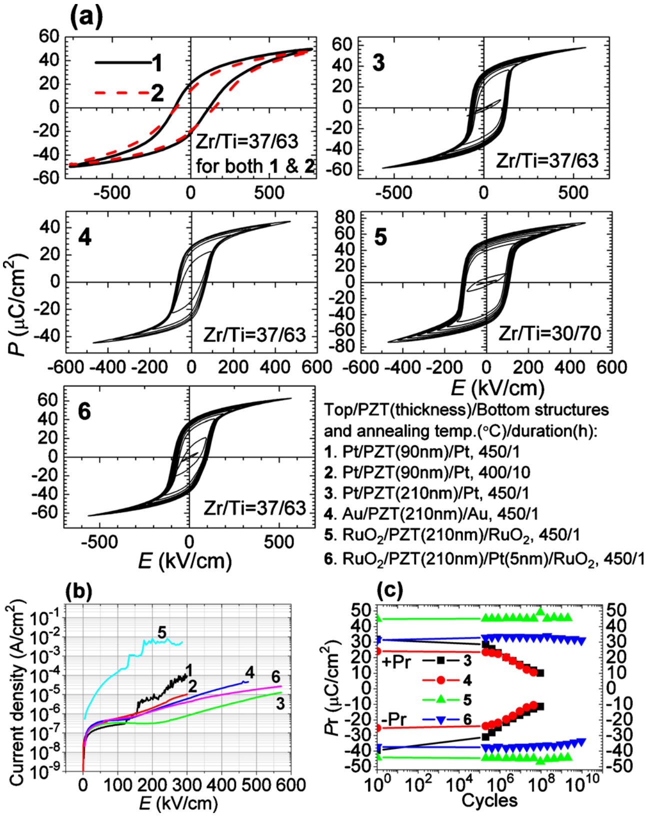

FIG. 3. (Color online) Properties of PZT films. (a) Polarization loops. (b) Leakage currents. (c) Fatigue curves. The samples' structures and annealing temperatures and durations are indicated in panel (a). In addition, for all the samples, each spin-coated layer was pyrolyzed at 210 °C, except for the last layer, which was only dried at 100–150 °C. The films were then annealed in air after being heated at 20 K/s in air (for 210 nm thick PZT) or N_2 (for 90 nm thick PZT).

zation, as suggested by microscope observations. Deceasing the thickness to 90 nm resulted in a significantly high leakage current and, consequently, failure in *P-E* measurement. Note that processing of PZT on RuO_2 is a big challenge even at high temperatures.[26] Further optimization is being conducted now. A compromise was made that employed a thin Pt layer (5 nm) between PZT and RuO_2, as reported for the high-temperature process.[26] PZT (Zr/Ti=37/63, same as on Pt and Au) buffered with a 6 nm thick layer of Zr/Ti =0/100 (sample 6) showed excellent properties in all aspects, with fatigue resistance tending to reach 10^{12} cycles (measured up to 10^{10} cycles) and lower leakage than the high-temperature samples.[26] Note that in previous studies on low-temperature processing, there was no effort to prepare PZT on RuO_2 or Pt/RuO_2, and no reported fatigue property. These results indicate device-quality of the films, and suggest suitability of the process for integrating PZT devices on other substrate materials (e.g., transparent glass) for low cost and novel applications.

In conclusion, a crystallization path that circumvents the formation of pyrochlore has been found for solution-deposited PZT films, which enables fabrication of device-quality ferroelectric films at low temperatures. The path is simply realized by applying a low pyrolysis temperature. This simple low-temperature path may open a new era in the long history of ferroelectric films, allowing low-cost, large-scale production, wider selection of device materials, and novel opportunities for interface engineering and device miniaturization because of suppressed diffusion.

[1] P. Muralt, R. G. Polcawich, and S. Trolier-McKinstry, MRS Bull. **34**, 658 (2009).

[2] N. Setter, D. Damjanovic, L. Eng, G. Fox, S. Gevorgian, S. Hong, A. Kingon, H. Kohlstedt, N. Y. Park, G. B. Stephenson, I. Stolitchnov, A. K. Taganstev, D. V. Taylor, T. Yamada, and S. Streiffer, J. Appl. Phys. **100**, 051606 (2006).

[3] C. A.-P. de Araujo, J. D. Cuchiaro, L. D. McMillan, M. C. Scott, and J. F. Scott, Nature (London) **374**, 627 (1995).

[4] B. H. Park, B. S. Kang, S. D. Bu, T. W. Noh, J. Lee, and W. Jo, Nature (London) **401**, 682 (1999).

[5] M. Aratani, T. Oikawa, T. Ozeki, and H. Funakubo, Appl. Phys. Lett. **79**, 1000 (2001).

[6] K. Maki, N. Soyama, S. Mori, and K. Ogi, Integr. Ferroelectr. **30**, 193 (2000).

[7] J. Perez, P. M. Vilarinho, and A. L. Kholkin, Thin Solid Films **449**, 20 (2004).

[8] K. Maki, B. T. Liu, Y. So, H. Vu, R. Ramesh, J. Finder, Z. Yu, R. Droopad, and K. Eisenbeiser, Integr. Ferroelectr. **52**, 19 (2003).

[9] M. Mandeljc, M. Kosec, B. Malic, and Z. Samardzija, Integr. Ferroelectr. **36**, 163 (2001).

[10] C. K. Kwok and S. B. Desu, J. Mater. Res. **8**, 339 (1993).

[11] A. Wu, P. M. Vilarinho, I. Reaney, and I. M. M. Salvado, Chem. Mater. **15**, 1147 (2003).

[12] Z. Wei, K. Yamashita, and M. Okuyama, Jpn. J. Appl. Phys., Part 1 **40**, 5539 (2001).

[13] C. H. Lu, W. J. Hwang, and Y. C. Sun, Jpn. J. Appl. Phys., Part 1 **41**, 6674 (2002).

[14] I. D. Kim and H. G. Kim, Jpn. J. Appl. Phys., Part 1 **40**, 2357 (2001).

[15] Z. J. Wang, H. Kokawa, H. Takizawa, M. Ichiki, and R. Maeda, Appl. Phys. Lett. **86**, 212903 (2005).

[16] A. Bhaskar, T. H. Chang, H. Y. Chang, and S. Y. Cheng, Thin Solid Films **515**, 2891 (2007).

[17] X. D. Zhang, X. J. Meng, J. L. Sun, T. Lin, and J. H. Chu, Appl. Phys. Lett. **86**, 252902 (2005).

[18] X. D. Zhang, X. J. Meng, J. L. Sun, T. Lin, J. H. Ma, J. H. Chu, N. Wang, and J. Dho, J. Mater. Res. **23**, 2846 (2008).

[19] M. L. Calzada, I. Bretos, R. Jiménez, H. Guillon, and L. Pardo, Adv. Mater. (Weinheim, Ger.) **16**, 1620 (2004).

[20] G. Garnweitner, J. Hentschel, M. Antonietti, and M. Niederberger, Chem. Mater. **17**, 4594 (2005).

[21] T. Morita and Y. Cho, Appl. Phys. Lett. **85**, 2331 (2004).

[22] See supplementary material at http://dx.doi.org/10.1063/1.3486462 for the details of experimental methods.

[23] A. Seifert, A. Vojta, J. S. Speck, and F. F. Lange, J. Mater. Res. **11**, 1470 (1996).

[24] M. C. Robinson, D. J. Morris, P. D. Hayenga, J. H. Cho, C. D. Richards, R. F. Richards, and D. F. Bahr, Appl. Phys. A **85**(2), 135 (2006).

[25] X. J. Lou, J. Appl. Phys. **105**, 024101 (2009).

[26] H. N. Al-Shareef, O. Auciello, and A. I. Kingon, J. Appl. Phys. **77**, 2146 (1995).

Downloaded 12 Sep 2010 to 150.65.164.25. Redistribution subject to AIP license or copyright; see http://apl.aip.org/about/rights_and_permissions